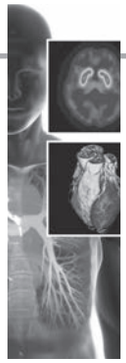

Diffusion-weighted MRI in head and neck cancer: experience to date and future potential

Imaging fulfills a crucial role in the work-up of patients with head and neck cancer, with its main tasks focusing on lesion characterization, staging, treatment planning and prognosis, as well as treatment follow-up. Diffusion-weighted MRI (DWI) measures differences in water mobility in the different tissue microstructures, which is influenced by cellular and vascular size, shape and density, as well as cellular membrane integrity. As such, the technique has the potential to differentiate tumoral tissue from normal tissue, inflammatory tissue and necrosis. Although DWI acquisition and evaluation still lacks standardization, the technique is rapidly developing and continuing to progress into clinical practice. This article aims to give an overview of the current use of DWI in head and neck cancer and discuss the (future) clinical applications.

KEYWORDS: characterization ■ diffusion-weighted MRI ■ head and neck cancer ■ staging ■ treatment follow-up

Vincent Vandecaveye*[1] & Frederik De Keyzer[1]

[1]Department of Radiology, University Hospitals Leuven, Herestraat 49, 3000 Leuven, Belgium
**Author for correspondence:*
Tel.: +32 16 340518
Fax: +32 16 343765
vincent.vandecaveye@uzleuven.be

Diffusion-weighted MRI (DWI) characterizes tissues based on the random Brownian displacement of water molecules, which is influenced by the underlying tissue specific microstructural hindrances. These random water molecule displacements are quantified by using the apparent diffusion coefficient that reflects the amount of signal loss on the DWI images, inversely correlated with tissue cellularity [1]. DWI is increasingly researched and applied in head and neck cancer with the aim of improving tumor detection and characterization and regional and distant staging, as well as the detection of tumor recurrence after treatment [2,3]. Technical issues caused by the high prevalence of air–tissue (susceptibility) boundaries and much lower water molecule density than in the brain have limited the introduction of DWI to the head and neck region until recent years. However, this has largely been overcome by technical improvements, such as the better shim gradients and more optimal shim calculations, stronger main magnetic fields, homogeneous high-quality imaging gradients, phased-array receiver coils and parallel imaging [4]. Although acquisition and evaluation of DWI still lacks standardization, it continues to progress into standard clinical imaging protocols. In this manuscript, we aim to give an overview of the major areas of development of DWI in head and neck cancer and (future) clinical applications.

Basic principles of DWI

Water molecules in biological tissues are confronted with tissue-specific mobility restriction, related to the presence of hindrances such as cell membranes, blood vessels and macromolecules. In biological tissue, water molecule displacements occur within and between the three major compartments: the intracellular space, the extravascular extracellular space and the intravascular space. With the DWI acquisitions that are currently most used, the mobility between the compartments and within the intracellular compartment is minimized, whereas the extracellular extravascular compartment is one of the main contributors to the DWI information. In solid malignant lesions, a higher cell density is seen, as well as cellular pleomorphism, larger cell volumes and higher prevalence of neoangiogenic vessels, all leading to a reduction of the mobility in the extracellular extravascular space and a subsequent restriction of the random water molecule movement. In tissues with low cell density, on the other hand, the extracellular extravascular space will be larger, leading to increased water proton mobility. This facilitation to movement occurs in inflammation (presence of interstitial edema) and in cystic/necrotic tissues, due to the lower interaction with cell membranes [5].

Usually, a T_2-weighted MRI sequence (e.g., a spin-echo echo-planar imaging sequence) is sensitized towards this water proton mobility by adding motion-probing gradients with a certain strength, indicated by the b-value. These gradients induce a signal loss in the images related to the strength of the motion-probing gradients and the amount and speed of water proton movement. By acquiring a range of

Future Medicine part of fsg

DWI images with different b-values, the average mobility can be quantified as the amount of signal loss with increasing b-values, which is called the apparent diffusion coefficient (ADC) and is expressed in mm²/s. Usually, a monoexponential fitting model is used to calculate the ADC value, according to the equation: $SI_i = SI_0 * \exp(-b_i * ADC)$, where SI_i is the signal intensity measured on the i'th b-value image and b_i is the corresponding b-value. SI_0 is a variable estimating the exact (without noise introduced at the time of the MR measurement) signal intensity for b = 0 s/mm². However, it is known that it is not only extracellular extravascular space mobility that contributes to the DWI signal, but also the water molecule movement inside blood vessels and tubular structures. Therefore, in recent years, there has been a shift to calculate not only the average water molecule mobility, but also to separate these so-called perfusion and true diffusion contributions, using a biexponential fitting procedure, first described by Le Bihan as the intravoxel incoherent motion approach. This approach fits the signal intensities with increasing b-value with a more advanced model ($SI_i = SI_0 x [(1-Fp)*\exp(-b_i*ADC_D) + Fp*\exp(-b_i*ADC_p)]$), yielding the separate true diffusion coefficient (ADC_D), the pseudo-perfusion mobility (ADC_p), and the perfusion fraction (Fp). The latter attempts to indicate the relative division of the total water molecule movement into the intravascular, or 'intrastructural', and the extracellular extravascular compartments, and is a value between 0 (only true diffusion contributions – pure extracellular extravascular components) and 1 (only perfusion contributions – pure intravascular components) [5].

In DWI images, hypercellular tissue, characterized by a limited extracellular extravascular space and subsequent restriction to water molecule movement, will only show limited signal decay with increasing b-value and present with persistently high signal intensity on the native DWI images with high b-value (e.g., 1000 s/mm² [b1000 images]) resulting in a low ADC. On the other hand, low cellularity tissues will have much more water proton movement, and will therefore show rapid signal decay with increasing b-value and present with low or absent signal intensity on the b1000 images resulting in a high ADC. As such, a combination of high signal intensity at high b-value images and low ADC is a typical presentation of a malignant lesion, which can be used to differentiate these from benign tissues that typically present with low signal on the b1000 images and high ADC.

However, this does not mean that tissues with high signal intensity on b1000 images are always malignant. In DWI, the extra motion-probing gradients are added to the underlying T_2-weighted sequence, which means that the signal intensity in each of the native b-value DWI images is influenced both by the original T_2-weighted signal and the motion-probing gradient-induced signal loss. If the signal intensity on b0 is very high, chances are that a hyperintensity at b1000 will remain, even in the case of a strong signal decay over the consecutive b-values (and a high ADC value, indicative of benign tissue). This remaining signal at b1000 is difficult to differentiate from a hyperintensity in malignant tissues with diffusion restriction. This effect is denominated as 'T2 shine-through', and it can be minimized by using higher b-values, but most often not completely avoided [6]. When in doubt whether the high signal intensity at b1000 is indicative of malignant tissue, it is therefore advised to perform an ADC calculation to filter out the areas of T2 shine-through. For the same reason, very low signal intensity at b0, nearly indistinguishable from the background noise, can be expected in fibrotic lesions including organized fibrosis, but also aggressive fibromatosis. In these cases, substantial signal decay over increasing b-values cannot be expected and ADC calculation should be considered as unreliable due to the low signal-to-noise ratio, and thus not performed or taken into account for lesion characterization (Figure 1).

Anatomy & image interpretation: general aspects

Before DWI images can be correctly interpreted, adequate knowledge of the normal diffusion-weighted anatomy in the head and neck is required. A number of structures have a variable physiological amount of impeded diffusion that should not be confused with tumoral lesions and may hamper the visual detection of tumoral lesions because of the increased background signal. These structures include the parotid and submandibular salivary glands, the thyroid gland, the palatine tonsils, normal lymph nodes, sebaceous cysts, the spine and the nerve roots of the brachial plexus. Contrary to this, the mucosal, submucosal, fatty and muscular tissue as well as blood vessels show complete signal loss on high b-value images. It is also beneficial for correct evaluation of DWI to always correlate the diffusion images with high-quality anatomical sequences.

The choice of b-values is pivotal to implement standardized clinical head and neck DWI as it largely impacts both qualitative and quantitative

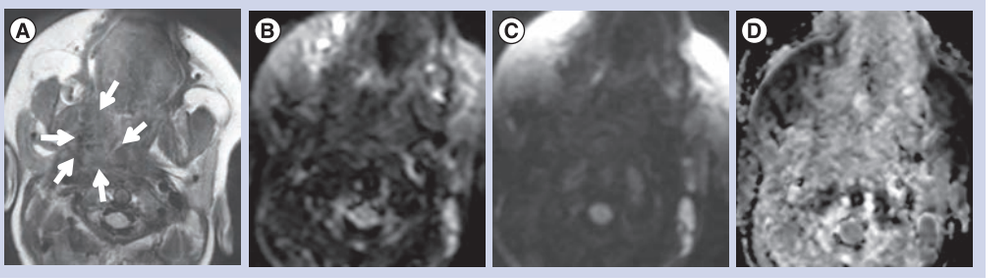

Figure 1. A 4-year-old infant presenting with a right oropharyngeal mass suspected of rhabdomyosarcoma. T_2-weighted MRI shows **(A)** ill-defined iso- to hypo-intense mass in the oropharynx (arrows). Neither diffusion-weighted **(B)** b0 nor **(C)** b1000 images show any detectable signal in the mass. As a result, **(D)** the apparent diffusion coefficient map only measures noise indistinguishable from the surrounding normal tissues. However, based on **(B & C)** the absent signal on native diffusion-weighted images, rhabdomyosarcoma can be excluded and the diagnosis of aggressive fibromatosis was suggested. This was confirmed by histopathology.

evaluation as well as reproducibility among different centers. Using low b-values, the sensitization towards fast moving molecules is maximized, resulting in images where the intravascular water molecules and very fast moving molecules in the extracellular extravascular space present with the strongest signal loss, while the slow moving spins will not have moved enough to induce a visible signal loss. The use of low b-values – usually between 0 and 100 s/mm^2 – results in ADC showing high values and reflects the effects of microperfusion and diffusion. Conversely, the application of high b-values – usually above 300 s/mm^2 – allows small water molecule movements to be perceived, maximizing the information provided by the molecule movements in the extracellular extravascular space [7]. Only applying these b-values above 300 s/mm² results in lower ADC values that more closely reflect the true diffusion of the tissue. The choice of the maximal b-value should be balanced between the signal-to-noise ratio and the ability to gain the largest specificity for the qualitative assessment of native DWIs and ADC calculation. Although data are not available for head and neck imaging, studies in liver DWI have shown that specificity of the technique improved with increasing maximal b-value. In our experience, we opt for a maximal b-value of 1000 s/mm^2, while a b-value of 500 s/mm^2 shows much lower conspicuity between malignant and benign tissues and should generally not be used as maximal b-value (Figure 2). As for other body regions, it is recommended in the literature to perform head and neck DWI with at least three b-values with maximum b-values exceeding 500 s/mm^2, to allow standardized ADC calculation [8]. At our institution, we use six b-values ranging between 0 and 1000 s/mm^2 (i.e., b0, b50, b100, b500, b750 and b1000). The use of multiple b-values holds a number of potential advantages. First, a higher number of b-values improves the accuracy of ADC calculations and can be used to minimize the influence of movement and noise error propagation. Second, in highly vascular tumors, the addition of nonzero low b-values can be used to appreciate vascular contributions that may falsely increase the total ADC value as there will be an additional, but variable, influence of microperfusion (flow-sensitive ADC) [7]. In our experience, this is useful to characterize and stage papillary thyroid cancers that have a highly hypervascular nature.

Qualitative analysis by single b-value DWI at a high b-value offers high sensitivity for the detection of tumoral disease, but may suffer from lower specificity [9]. This is particularly relevant for assessing lymph nodes, where benign lymph nodes cannot reliably be distinguished from metastatic lymphadenopathies on high b-value images alone and require, at least, visual assessment of the ADC map. Generally, tumoral tissue appears as hyperintense on high b-value images and low intensity on the ADC map, while necrosis and apoptosis appear as low signal on high b-value images and high intensity on the ADC map. In the postradiotherapy setting, a significantly higher b1000 signal intensity was found for recurrent primary tumors compared with post-chemoradiotherapy (CRT) necrosis and inflammation, and the bright signal of tumoral lesions on the b1000 images allows for first-line qualitative evaluation for detection of potentially suspicious lesions [10]. In our experience, combining b1000 images with anatomical sequences and/or dynamic contrast-enhanced sequences allows millimeter primary or recurrent tumors, often too small to perform reliable ADC quantification, to be reliably detected and characterized. Visual assessment of the morphological appearance of

lesions at native DW images is often underestimated in the literature and should be a mandatory part of lesion evaluation. Rim-like or nodular b1000 signal heterogeneity in correlation with anatomical images is a reflection of tumor heterogeneity in partially necrotic and fibrotic lesions. In addition, small necrotic foci in micrometastatic head and neck squamous cell carcinoma (HNC) can only be visible at low b-values and remain undetected at high b-values or ADC (Figure 3). Therefore, qualitative evaluation should ideally include the visual assessment of b0, b1000 images and the ADC map. Quantification by means of ADC is the most common method of analysis of head and neck lesions next to visual assessment. In current clinical practice, ADC quantification is mostly carried out by manual region of interest (ROI) delineation over the tissue of interest (primary tumor – lymph node) with basic descriptive analysis performed over the delineations (e.g., mean, median, standard deviation and range). More advanced analysis methods, including histogram analysis or voxel-by-voxel evaluation using the functional diffusion map and parametric response maps, are not yet in the stage of clinical practice [11]. ROIs are in general placed over the entire lesion; however, when obvious solid and necrotic components are visible on the native b1000 images or ADC maps, ROIs should be placed on the distinct tissues separately [8,12]. Importantly, currently neither the standardized acquisition method nor the standardized threshold has been defined for ADC-based lesion characterization. Also, insufficient data exist to conclude that ADC cutoff values obtained at 1.5 Tesla (T) can be directly transferred to 3 T DWI evaluations or that ADC values are directly interchangeable between different vendors and scanner hardware [13].

Clinical application: tumor characterization

A number of studies have reported on the ability of DWI to differentiate benign from malignant lesions in the head and neck, with the ADC of benign lesions being consistently higher than these of malignant lesions [4,13,14]. However, considering the broad range of both malignant and benign histological entities in the head and neck, it is unlikely that a generalized use of ADC with a single determined threshold is feasible for lesion differentiation. Therefore, DWI for tissue characterization should be used in specific indications, tumor sites and pathology [11,15]. DWI may be of value for lesion differentiation at the primary site, such as the thyroid and salivary glands and the tonsillar ring that usually do not allow adequate characterization based on conventional imaging

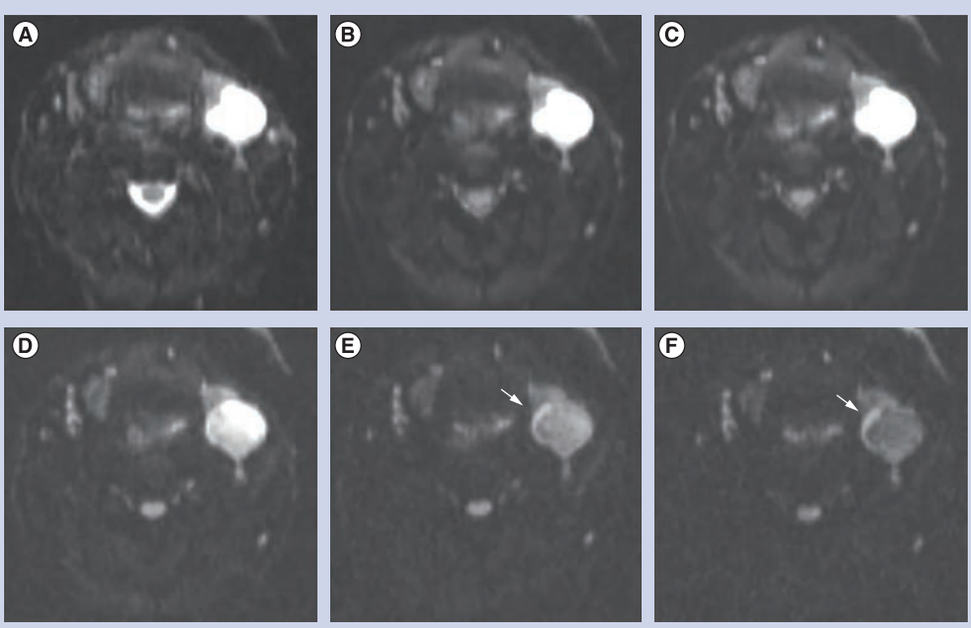

Figure 2. Partially necrotic lymphadenopathy in the left neck with viable tumor tissue in the periphery of the lesion. Diffusion-weighted images at **(A)** b0, **(B)** b50, **(C)** b100 and **(D)** b500 do not allow the viable component to be accurately distinct from the necrotic component. However, the images at **(E)** b750 and **(F)** b1000 allow visual differentiation, with the necrotic area showing loss of signal in the center and the viable component appearing as a hyperintense area in the lesion periphery (arrows).

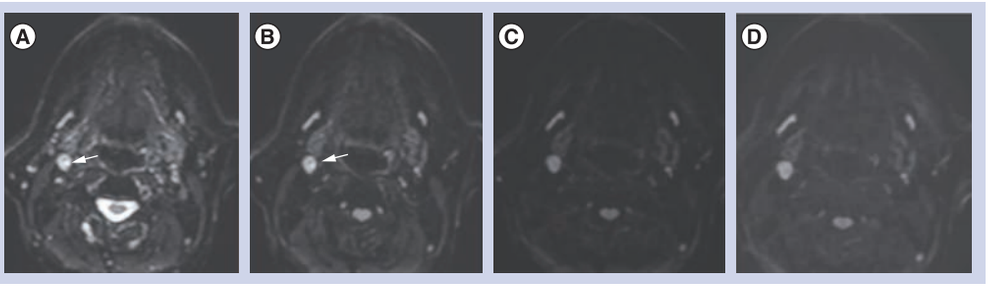

Figure 3. Small lymph node in the right neck in a patient with a history of surgically treated small oral cancer. The diffusion-weighted **(A)** b0 image shows a small hyperintense focus in the lymph node (arrows), which is still visible at **(B)** b100. However, no focal hyperintensity can be seen at **(C)** b750 or **(D)** b1000. This is suggestive of a small necrotic focus representing a small metastatic node and was confirmed by histopathology after surgical resection.

alone and need additional biopsy. Moreover, DWI may be of value for tumor characterization in patients presenting with lymphadenopathy, but without a clear primary tumor.

A recent study showed that tonsillar HNC showed significantly higher mean ADC of 0.933×10^{-3} mm^2/s (range: 0.789–1.175×10^{-3} mm^2/s) compared with normal tonsil, showing a mean ADC of 0.814×10^{-3} mm^2/s (range: 0.548–1.312×10^{-3} mm^2/s) [16]. Similarly, DWI has shown value to differentiate HNC from lymphoma in primary site lesions that are indeterminate at conventional imaging where HNC showed significantly higher ADC of $0.96 \pm 0.11 \times 10^{-3}$ mm^2/s, compared with $0.65 \pm 0.09 \times 10^{-3}$ mm^2/s for lymphoma (Figure 4) [17]. Both at the primary site [18] and neck lymphadenopathies, HNC has shown significantly higher ADC compared with lymphoma and nasopharyngeal carcinoma (NPC) [19–21]. Although acceptable accuracies may be obtained to discriminate the respective tumors, overlap of ADC on an individual base may limit its use. Usually DWI allows for reliably differentiating HNC from lymphoma or NPC, but an ADC-based separation of lymphoma and NPC is more difficult due to overlapping values [19]. This is probably due to the more pronounced histological similarity between NPC and lymphoma, whereas HNC has a clearly different tissue cellularity and cell size, and more frequent necrotic degeneration [19]. Importantly, differentiating lymphoma from HNC can currently only reliably be performed in non-Hodgkin lymphoma, as the higher ADC found in Hodgkin lymphoma may overlap with the ADC of HNC [19,20].

Although ultrasound is the standard imaging modality for the evaluation of thyroid nodules, the technique does not allow reliable lesion characterization. As such, ultrasound-guided fine needle aspiration cytology (FNAC) has become the standard in oncologic screening of thyroid nodules, and proved to have a very low false-positive rate, but may suffer from an increased false-negative rate in case of low cellularity in the FNAC sample [22]. As such, thyroidectomy cannot always be avoided in case of negative findings after FNAC or intensive follow-up may be required in equivocal cases. A number of studies have shown the ability of DWI to differentiate benign from malignant thyroid nodules, with reported sensitivities between 85 and 100% and specificities between 100 and 79% [23–27]. However, it is quite hard to compare these studies, as most used the absolute lesion value while one study used the relative difference between lesion and surrounding thyroid tissue for lesion characterization. Moreover, the studies reporting absolute ADC values for lesion differentiation used different b-value settings, making it currently impossible to advocate a clear ADC threshold for routine clinical applications in thyroid gland lesions. In addition, it is unclear whether DWI will be able to detect small tumoral foci arising from benign (follicular) nodules. DWI could possibly be used in the further differentiation of cold thyroid nodules, incidentally discovered thyroid nodules or nodules with indeterminate cytology [11].

Similarly, DWI may help to differentiate and avoid invasive diagnostic procedures in salivary gland lesions, which now – as a rule – require ultrasound-guided FNAC or biopsy for definitive characterization. Initially, good results were obtained using absolute ADC values, with high ADC correlating with benign lesions and low ADC correlating to malignant lesions based on a fixed threshold [28]. However, these results could not be confirmed in a later and larger study [29]. One of the major problems in DWI of the salivary gland using absolute ADC values is the multitude of histological entities in both the benign and malignant spectrum of lesions. For instance, considering their histological background with variable amounts of lymphoid tissue and germinal centers, benign

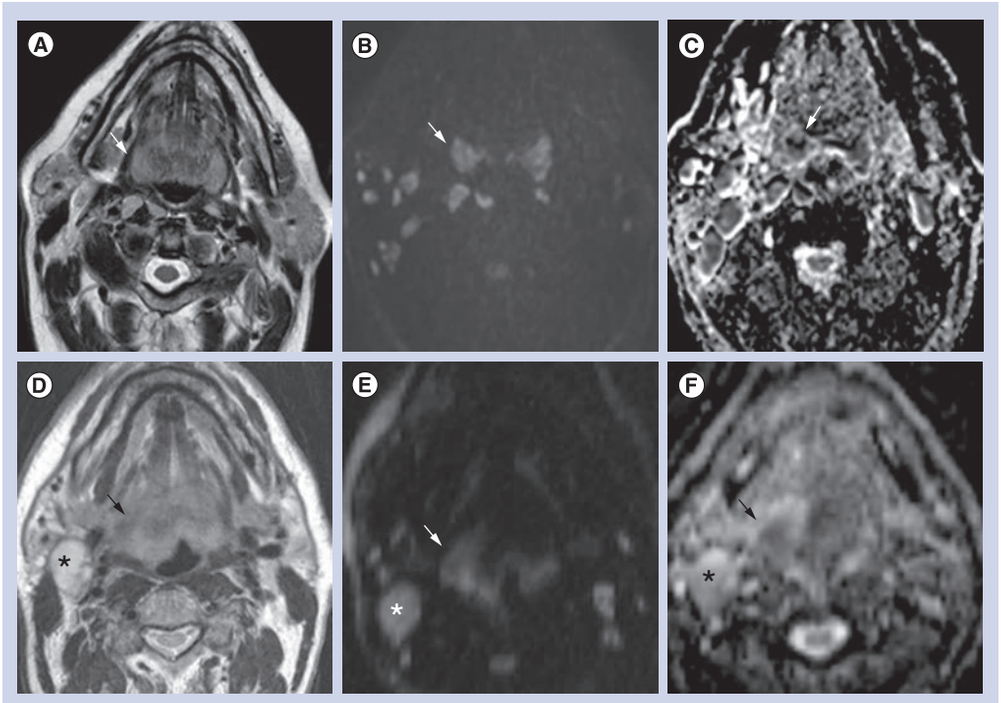

Figure 4. A patient with painless swelling of the right tonsil and a patient with a lump in the right neck. (A) On the T_2-weighted MR image, the right tonsil appears slightly hypointense, but is hyperintense (arrow) at **(B)** b1000 (arrow) and correlates to a **(C)** low apparent diffusion coefficient of 0.00069 mm²/s (arrow). This corresponds to a histopathologically proven non-Hodgkin lymphoma. **(D–F)** Another patient presenting with a lump in the right neck. **(D)** MRI shows lymphadenopathy in the right neck (asterisk) and a right oropharyngeal mass (arrow). The oropharyngeal mass is hyperintense (arrow) at **(E)** b1000 and correlates to **(F)** an apparent diffusion coefficient of 0.00095 mm²/s (arrow), which corresponded to a histopathologically proven squamous cell carcinoma.

Warthin tumors show low ADC values that are indistinguishable from malignant lesions. Nevertheless, DWI may be useful in specific settings or indications as it reliably allows differentiating pleomorphic adenomas from malignant tumors [30]. However, it remains questionable to what extent this may impact patient management as pleomorphic adenomas – known to have risk of malignant transformation – are usually surgically resected. Currently, attempts are still being made to improve the diagnostic accuracy of DWI for the differentiation of salivary gland tumors. In combination with perfusion MRI, the diagnostic accuracy of DWI can be improved by applying a specific ADC threshold to a specific washout pattern, enabling a better differentiation of Warthin tumors from carcinomas or pleomorphic adenomas from carcinomas [31]. Also, in a recent publication, the intravoxel incoherent motion approach (see above) was used to differentiate benign from malignant tumors (based on ADC) and Warthin tumors from pleomorphic adenoma (based on Fp) [32]. A combination of the intravoxel incoherent motion parameters even allowed a discriminatory accuracy of 100% to be reached between the three examined lesion types.

Clinical application: nodal staging

Except for a few studies [21,33], it is generally accepted that metastatic lymph nodes of HNC have significantly lower ADC compared with benign lymph nodes [20,34–37]. The contradicting results in one of the first studies compared with the others is likely attributable to the different set of b-values used, different included number of necrotic metastases (up to 48% in the study of Sumi *et al.* [21]) and selection of the ROI for ADC calculation. Similar to most other DWI applications, this again stresses the need for standardization in both imaging technique and interpretation, which are currently lacking. However, recent studies that used identical b-value settings ranging from b0 to b1000 s/mm² obtained similar accuracy with no or only minimal variability between thresholds used (ranging between 0.94×10^{-3} and 1.03×10^{-3} mm²/s).

Described sensitivities range from 83 to 98%, with specificities ranging between 97 and 87% [20,34–37]. The additional value of DWI to conventional imaging lies mainly in an improved sensitivity for detecting subcentimetric lymphadenopathies, which was shown to be 76% for DWI, compared with 7% for conventional

imaging in a previous study; be it at the cost of a diminished specificity due to false positives in reactive or granulomatous/infectious lymph nodes [35]. Contrary to this, necrosis can falsely increase ADC and lead to false-negative readings. As previously mentioned, visual inspection of native DWI images is mandatory to assess possible nodal heterogeneity due to necrosis and the correlation with conventional imaging sequences [20,38].

It is important to note that to date DWI has not been researched to evaluate the N0 neck, and is therefore not advocated in this setting. The inability of the technique to detect micrometastases smaller than 4 mm makes DWI unfit for ruling out small nodal metastases, and thus obviate neck dissection. However, preliminary findings do suggest a possible role of DWI for presurgical evaluation of the node positive neck to reliably detect or exclude contralateral nodal metastases in tumors extending or close to the midline or help in the detection of level IV skip metastases in oral cancer [35]. For radiotherapy planning, a previous study has shown a closer conformity between nodal staging by DWI with pathological staging then anatomical imaging, which could potentially result in a decreased treatment-induced toxicity or intensified treatment on small tumor deposits undetected by conventional imaging [39]. This mainly involves assessment of the contralateral neck. Moreover, as DWI can reliably exclude metastatic disease in lymph nodes larger than 4 mm, DWI may be used to reduce the tissue volume with high-dose radiation that would have been included based on current treatment guidelines or conventional imaging [40]. Applications that may benefit from this ability include unilateral or parotid-sparing 3D conformal radiation therapy, as in those cases the contralateral site is irradiated with lower elective radiation doses than conventionally used [41,42].

Clinical application: prediction of treatment outcome

The value of DWI as an early surrogate biomarker for treatment outcome is under investigation. Assessment of the tumor properties prior to and tumoral changes early on during the course of (chemo)radiation by DWI is gaining more and more interest as the differences between inflammatory changes and tumor are quite straightforward and DWI imaging should, therefore, be reliably applicable at the early stages of treatment. The ability to predict later tumor response may help to plan or modify treatment on an individual response basis, aiming to improve treatment efficiency and decrease unnecessary toxic side effects. The development of targeted treatments, radiosensitizers and intensity-modulated radiation therapy make treatment planning more complex and require reliable bioadaptive imaging modalities for optimal planning. It should be noted, however, that despite the promising results in the literature for treatment prediction, DWI cannot be readily applied for radiotherapy planning or adaptive treatment as the topographical information contained in the DWI images and ADC map is usually not correct due to the inherent susceptibility-induced distortion artifacts. DWI images first need to be corrected for these distortions using nonrigid registration, which was performed using a six-step multiresolution strategy based on mutual information, a gradient-based optimizer and a global smoothness penalty in a recent study [43]. Second, the distortion-corrected DWI images should be rigidly registered to the planning CT [43]. It seems evident that at this stage, this cannot be implemented in the routine clinical setting and requires further development and collaboration between radiologists, radiotherapists and medical engineers or physicists.

Currently, limited data are available regarding the use of DWI as a pretreatment imaging biomarker. It is generally accepted that tumors with a low ADC value prior to treatment have a better treatment outcome than patients with increased ADC. Although the underlying biophysical rationale has not been proven, it is presumed that tumors with higher ADC are more necrotic and may correlate with decreased tumor perfusion and increased hypoxia, which have an adverse effect on treatment efficacy. In previous studies, tumors with a low pretreatment ADC value had significantly greater tumor regression 2 weeks after neoadjuvant treatment and correlated significantly with complete clinical or pathological remission after definitive chemoradiation, while lesions with high ADC show significant likelihood of nonresponse or tumor recurrence during follow-up [44,45]. Contrary to this, in a study including 50 patients with primary and nodal tumors and a follow-up of 22 months, pretreatment ADC showed no predictive value [46]. The discrepancies found between these studies could introduce difficulties in the accurate implementation of pretreatment ADC for treatment decisions in individual patients. Overcoming these problems might be feasible by using a combination of ADC values before and during treatment or by applying ADC histograms of the entire tumor to depict the heterogeneity of the lesion. In a recent study, ADC histograms showed modest predictive

value in a small patient population, warranting further evaluation [47].

A number of studies have evaluated early DWI response assessment during chemoradiation. Two initial studies in 40 and 30 patients, respectively, demonstrated that ADC changes between baseline and 1, 2 and 4 weeks during chemoradiation follow-up scan were significantly lower in tumors with later recurrence than in tumors with complete remission [12,44]. In these studies, the sensitivities ranged between 86 and 100% and specificities between 83 and 96%, and the ADC change proved to be an independent predictor of 2-year locoregional control [12]. Another study in 41 patients showed that serial ADC changes from pretreatment, over intratreatment to post-treatment were highly predictive of locoregional failure [46]. When using an early or late ADC decrease as a discriminating parameter, a sensitivity of 80% and specificity of 100% was obtained for predicting locoregional failure. Lesions without ADC decrease during serial ADC measurements were unlikely to show locoregional failure during the first 6 months of follow-up. The described ADC decrease probably indicates tumor repopulation, which is supported by historadiological correlation in animal-based studies [48,49].

Currently, the optimal time point for early response assessment by DWI remains to be determined, but is likely to be within the first 4 weeks after the start of treatment. As for other DWI applications, thresholds have not yet been standardized. Further technical advances have to be taken into account, however, including the possibility that mean ADC changes from entire tumor delineations may be abandoned in the future as they are unlikely to detect small treatment-resistant intratumoral deposits that may eventually determine the patient's outcome. As previously mentioned, this can be overcome by delineation of the tumoral ROI based on the b1000 tumor heterogeneity, although this could lead to increased interobserver variability. Histogram analysis and parametric response maps, which have the ability to depict the spatial distribution or heterogeneity of tumor response, may further enhance the technique's ability for early response assessment [50,51]. In a study performing response assessment at 2 weeks after the start of chemoradiation in 30 patients, whole tumor ADC histograms were analyzed, and mean ADC, kurtosis, skewness and their respective percentage changes were correlated to 2-year local control [50]. Tumors with local failure showed a significantly smaller percentage increase in mean ADC, a higher skewness and higher kurtosis compared with tumors with local control. These parameters were also predictors of local failure, but not independent from tumor volume. Another study in 15 patients on DWI-based response assessment at 3 weeks during chemoradiation used a parametric response map to evaluate serial changes on spatially-aligned ADC maps (PRMADC) [51]. The study showed significant differences in PRMADC between responders and nonresponders at pathologic examination, while mean ADC changes did not show any correlation.

Clinical application: detection of tumor recurrence

Next to its antitumoral effects, (chemo-)radiation also induces edema, fibrosis and inflammation of the normal surrounding tissue, leading to important signal intensity changes that may hamper the early detection of tumor recurrence by conventional imaging. Also, necrosis may occur, which cannot consistently be differentiated from tumor recurrence by CT nor conventional MRI. Fluorodeoxyglucose (FDG)-PET can in part overcome this problem, but its accuracy may be diminished given the FDG uptake in inflammatory tissue, causing false-positive findings or hampering the detection of small tumoral foci against an inflammatory background.

Due to its mechanism of signal generation, DWI may be well suited for detecting tumor recurrence – with high cellularity, high restriction and low ADC – contrasting with the background of inflammation and interstitial edema – with low cellularity, low restriction and high ADC.

Two initial studies showed the value of DWI for detecting post-treatment HNC both in the early and late post-treatment phase (>4 months to <4 months post-CRT) [10,52] and showed high sensitivity (84–94%) and specificity (90–95%). Of note, both studies were independently published within a few months' time and obtained an identical threshold of 0.0013 mm^2/s, indicating the potential reproducibility of the technique. The findings of these initial studies was recently confirmed by a study in post-treatment laryngeal and hypopharyngeal cancer [53]. Using a threshold of 0.0013 mm^2/s, mono-exponential ADC analysis yielded a sensitivity of 67% and specificity of 86%. Importantly, qualitative DWI combined with morphological imaging showed the highest sensitivity of 94% and specificity of 100% [53]. Possible reasons for the larger overlap of ADC between malignant and benign lesions and lower accuracy were mainly

attributed to the more challenging imaging site prone to artefacting and overall smaller tumor size. False-positive and false-negative ADC measurements can occur due to partial volume effects in small structures, diffuse fibrosis or diffuse necrosis with only scattered small viable tumor components. This finding stresses the importance of qualitative DWI assessment and the need for coregistered anatomical imaging as reference. As the b1000 signal intensity correlated significantly with the presence of recurrent tumors, the need for ADC quantification can be diminished in the post-CRT phase, especially in small lesions difficult to measure by ADC [10].

Although findings need to be confirmed in larger multicenter trials, the high negative predictive value of DWI – already in the early post-treatment phase – may help to select patients in whom elective post-treatment neck dissection can be obviated even in the case of persistent lymph nodes or also in the case of recurrent or persistent lesions at the primary site, where the differentiation between radionecrosis and tumor recurrence is pivotal. This may be especially valuable in cases where CT or FDG-PET/CT findings are expected to be equivocal.

Additionally, due to the high sensitivity and improved background suppression, DWI may be particularly useful for the early detection of small recurrent tumors, which may lead to an improved patient survival by increasing the therapeutic window for salvage surgery [54]. This may be of particular importance in oropharyngeal cancer where the therapeutic window for salvage surgery may be narrow as operability will not only be determined by the ability to obtain oncologic control, but also functional preservation and surgical reconstructive options [54]. In addition, owing to its improved lesion conspicuity, DWI may be of additional value as a presurgical staging tool. With the advent of chemoradiation, isolated nodal recurrence has become a quite rare event. Therefore, concurrent persistence of the primary site should often be suspected [55]. DWI may be helpful in the evaluation of a possible persistent small primary tumor in the case of persistent or recurrent lymphadenopathy and help to guide the need for additional laryngoscopy and surgical planning (Figure 5) [10]. In short, the technique may have value as a second-line characterization tool to facilitate patient management in the case of persistent lymph nodes or primary lesions that are equivocal for tumor recurrence or necrosis based on conventional imaging as well as a staging tool prior to salvage surgery.

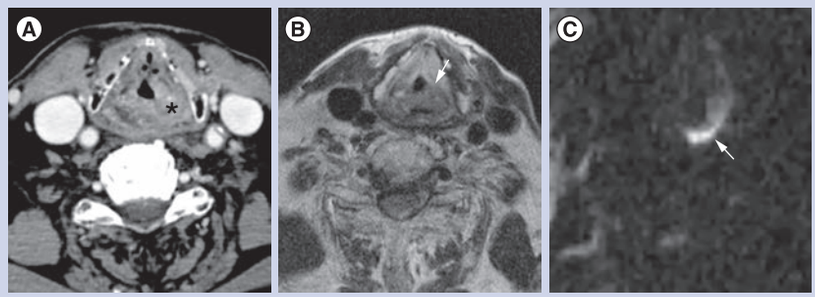

Figure 5. Patient with increasing hoarseness 8 months after chemoradiation for laryngeal cancer. A total of 8 months after chemoradiation for laryngeal cancer, **(A)** the CT scan shows a suspect mass in the left retro–arytenoid region (asterisk). However, this could not be confirmed by histopathology after endoscopy under anesthesia. Subsequent MRI including **(B)** T_2-weighted imaging showed a hypointense mass (arrow), with a corresponding strong hyperintensity on **(C)** the b1000 diffusion-weighted image (arrow), compatible with tumor recurrence. Repeat biopsy was performed, confirming the tumoral recurrence.

Whole body DWI

Technological progress has enabled the application of time-efficient whole body (WB)-DWI with thin-slice acquisition and multiplanar image reformatting, while at the same time reducing fat and susceptibility-related artifacts, WB-DWI harbors potential advantages to anatomical and metabolical imaging. Its high contrast and spatial resolution improves detection of lymphadenopathy and visceral metastases, irrespective of lesion size and in complex anatomical sites. As a rule, correlation to anatomical WB sequences is mandatory, as well as the inclusion of high-resolution, thin-slice breath-hold sequences over the lungs given the lower sensitivity of DWI for detecting lung metastases. Currently, only a limited number of studies have investigated WB-DWI for staging head and neck cancer. In a study including 70 patients with postoperative differentiated thyroid cancer, WB-DWI was compared with FDG-PET/CT and ^{131}iodine WB scintigraphy. On a per-patient basis, detectability of metastases was 67.1% for ^{131}iodine WB scintigraphy, 84.2% for FDG-PET and 57.6% for WB-DWI. However, WB-DWI showed additional value for detecting skeletal metastases. Importantly, both restriction on DWI and FDG positive signal on FDG-PET were predictors of lower survival chances [56].

In a study including 150 patients with untreated NPC, WB-MRI showed similar sensitivity (77.8 vs 72.2%; $p > 0.999$) and specificity to FDG-PET/CT (98.5 vs 97.7%; $p > 0.999$) [57]. The same group found that in a study including 179 NPC patients at high risk of residual or recurrent nasopharyngeal carcinoma, WB-MRI also showed similar sensitivity (90.9 vs 87.3%; $p = 0.69$) and specificity (91.1

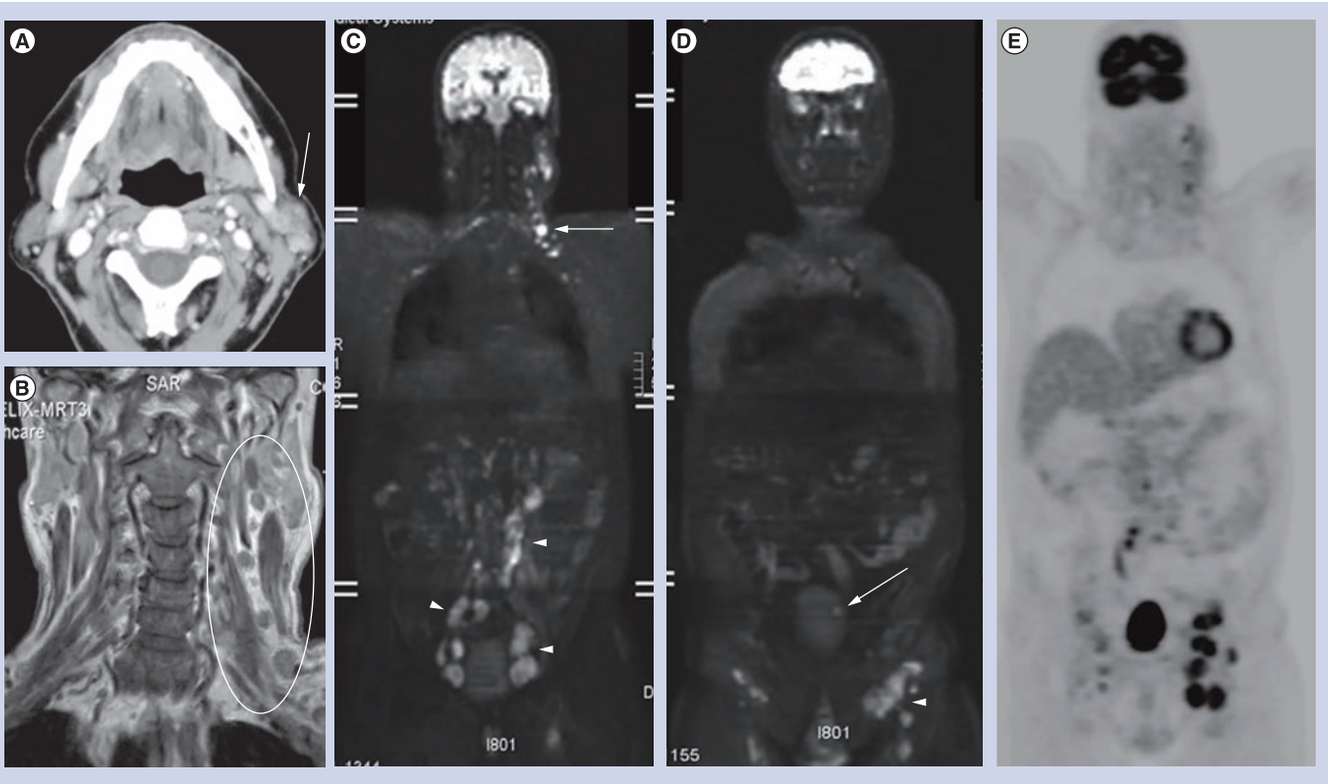

Figure 6. Patient suspected of left parotid tumor. (A) CT shows suspect left parotid mass (arrow) with **(B)** multiple lymphadenopathies in the left neck on the subsequent MRI (oval). **(C & D)** Whole body diffusion-weighted MRI at b1000 confirms the lymphadenopathies in the left neck (arrows), but also shows multiple lymphadenopathies in the retroperitoneum, bilateral iliac chains and bilateral in the groin (arrowheads). Moreover, the whole body diffusion-weighted MRI at b1000 also shows **(D)** a small hyperintense lesion in the bladder wall (arrow). **(E)** On fluorodeoxyglucose PET, the multifocal lymphadenopathies are confirmed, but the small bladder lesion is obscured by renal excretion of fluorodeoxyglucose in the bladder (also not apparent on the CT – data not shown). Cystoscopy with biopsy and nodal biopsy confirmed the presence of transitional cell cancer of the bladder with diffuse dissemination to the lymph nodes and left parotid gland.

vs 90.3%; p > 0.99) compared with FDG-PET/CT [58]. WB-MRI may, therefore, be useful as a first-line screening tool providing comprehensive evaluation of locoregional and distant disease in one examination. Evidently, WB-DWI or WB-MRI are still relatively new concepts that still require further clinical validation before routinely implemented (Figure 6).

Conclusion

DWI introduced a novel contrast into the head and neck imaging modalities based on the differences in water molecule mobility. In this way, DWI provides information on the tumoral microstructure that is supplemental to anatomical and metabolic imaging.

Future perspective

Although recent years have seen a shift of DWI into clinical practice in most oncologic applications, standardization and comparison between centers is still lacking, which is only being addressed slowly. However, many studies have already shown the large clinical potential of this technique for lesion characterization, nodal staging, pre- and intra-treatment outcome prediction, and recurrence detection in HNC. Nevertheless, future studies should further aim at comparing and integrating head and neck DWI with other functional modalities such as PET/CT and PET/MRI. DWI has the added benefits of being easy to add to a routine MR examination and does not require the use of exogenous contrast agent. It will certainly integrate further into clinical routine in the following years.

Financial & competing interests disclosure

The authors have no relevant affiliations or financial involvement with any organization or entity with a financial interest in or financial conflict with the subject matter or materials discussed in the manuscript. This includes employment, consultancies, honoraria, stock ownership or options, expert testimony, grants or patents received or pending, or royalties.

No writing assistance was utilized in the production of this manuscript.

Executive summary

Background

- Diffusion-weighted MRI (DWI) is increasingly researched and applied in head and neck cancer with the aim of improving tumor detection and characterization, regional and distant staging, as well as the detection of tumor recurrence after treatment.

Basic principles of DWI

- DWI characterizes tissues based on the random Brownian displacement of water molecules, which is influenced by the underlying tissue-specific microstructural hindrances.
- By acquiring a range of DWI images with different b-values, the average mobility can be quantified as the amount of signal loss with increasing b-values, which is called the apparent diffusion coefficient (ADC) and is expressed in mm^2/s.
- In DWI images, hypercellular tissue will show persistent high signal intensity on the native DWI images with a high b-value (e.g., 1000 s/mm^2 [b1000 images]) and low ADC.
- Low cellularity tissues present with low or absent signal intensity on the b1000 images and high ADC.

Anatomy & image interpretation: general aspects

- Knowledge of anatomical structures with physiologically impeded diffusion and correlation to anatomical images is mandatory for correct image interpretation.
- The choice of b-values is pivotal to implement standardized clinical head and neck DWI.
- Combining qualitative analysis of high b-value images with anatomical sequences and/or dynamic contrast-enhanced sequences allows reliable detection and characterization of millimeter primary or recurrent tumors, often too small to perform reliable ADC quantification.
- Quantification by means of ADC is the most common method of analysis of head and neck lesions next to visual assessment.
- More advanced analysis methods, including histogram analysis or voxel-by-voxel evaluation using the functional diffusion map and parametric response maps, are currently not yet in the stage of clinical practice.

Clinical application: tumor characterization

- DWI may be of value for lesion differentiation at the primary site, such as the thyroid and salivary glands and the tonsillar ring, that usually do not allow adequate characterization based on conventional imaging alone and need additional biopsy.
- DWI may be of value for detecting unknown primary tumors in patients presenting with lymphadenopathies.

Clinical application: nodal staging

- Metastatic lymph nodes of head and neck squamous cell carcinoma have generally significantly lower ADCs compared with benign lymph nodes.
- The additional value of DWI to conventional imaging lies mainly in an improved sensitivity for detecting subcentimetric lymphadenopathies.
- DWI has not yet been researched to evaluate the N0 neck, and is therefore not advocated in this setting.

Clinical application: prediction of treatment outcome

- Currently, limited data are available regarding the use of DWI as a pretreatment imaging biomarker. Tumors with a low ADC value prior to treatment have better treatment outcome than patients with increased ADC.
- For early DWI response assessment, patients with initial substantial ADC increase during treatment have better treatment outcome than patients with absent or minimal AD change.
- Optimal time windows for early response assessment are between 2 and 4 weeks during chemoradiation or 3 weeks after the end of chemoradiation.

Clinical application: detection of tumor recurrence

- Due to its mechanism of signal generation, DWI is well suited for detecting tumor recurrence – with high cellularity, high restriction and low ADC – contrasting with the background of inflammation and interstitial edema – with low cellularity, low restriction and high ADC.
- As the b1000 signal intensity correlates significantly with the presence of recurrent tumor, the need for ADC quantification can be diminished in the postchemoradiotherapy phase, especially in small lesions difficult to measure by ADC.

Whole body DWI

- Correlation to anatomical whole body sequences is mandatory, as well as the inclusion of high resolution, thin slice breath hold sequences over the lungs given the lower sensitivity of DWI for detecting lung metastases.
- In thyroid cancer, whole body DWI shows additional value for detecting bone metastases while restrictive whole body DWI is a predictor of low survival.
- For nasopharyngeal cancer, whole body MRI shows similar accuracy to metabolic imaging for distant staging while allowing more detailed depiction of locoregional disease extent. The technique may, therefore, be useful as a first-line screening tool providing comprehensive evaluation of locoregional and distant disease in one examination.

Conclusion

- In the head and neck, DWI provides information on the tumoral microstructure that is supplemental to anatomical and metabolic imaging.

Future perspective

- DWI is moving into clinical practice in most oncologic applications, but standardization and comparison between centers is still lacking.

References

1 Ross BD, Moffat BA, Lawrence TS *et al*. Evaluation of cancer therapy using diffusion magnetic resonance imaging. *Mol. Cancer Ther.* 2(6), 581–587 (2003).

2 Yoshikawa K, Nakata Y, Yamada K, Nakagawa M. Early pathological changes in the parkinsonian brain demonstrated by diffusion tensor MRI. *J. Neurol. Neurosurg. Psychiatry* 75(3), 481–484 (2004).

3 Eastwood JD, Lev MH, Wintermark M *et al.* Correlation of early dynamic CT perfusion imaging with whole-brain MR diffusion and perfusion imaging in acute hemispheric stroke. *AJNR Am. J. Neuroradiol.* 24(9), 1869–1875 (2003).

4 Wang J, Takashima S, Takayama F *et al.* Head and neck lesions: characterization with diffusion-weighted echo-planar MR imaging. *Radiology* 220(3), 621–630 (2001).

5 Le Bihan D, Breton E, Lallemand D, Aubin ML, Vignaud J, Laval-Jeantet M. Separation of diffusion and perfusion in intravoxel incoherent motion MR imaging. *Radiology* 168(2), 497–505 (1988).

6 Koh DM, Collins DJ. Diffusion-weighted MRI in the body: applications and challenges in oncology. *AJR Am. J. Roentgenol.* 188(6), 1622–1635 (2007).

7 Thoeny HC, De Keyzer F, Vandecaveye V *et al.* Effect of vascular targeting agent in rat tumor model: dynamic contrast-enhanced versus diffusion-weighted MR imaging. *Radiology* 237(2), 492–499 (2005).

8 Padhani AR, Liu G, Koh DM *et al*. Diffusion-weighted magnetic resonance imaging as a cancer biomarker: consensus and recommendations. *Neoplasia* 11(2), 102–125 (2009).

9 Takahara T, Imai Y, Yamashita T, Yasuda S, Nasu S, Van Cauteren M. Diffusion weighted whole body imaging with background body signal suppression (DWIBS): technical improvement using free breathing, STIR and high resolution 3D display. *Radiat. Med.* 22(4), 275–282 (2004).

10 Vandecaveye V, De Keyzer F, Nuyts S *et al.* Detection of head and neck squamous cell carcinoma with diffusion weighted MRI after (chemo) radiotherapy: correlation between radiologic and histopathologic findings. *Int. J. Radiat. Oncol. Biol. Phys.* 67(4), 960–971 (2007).

11 Thoeny HC, De Keyzer F, King AD. Diffusion-weighted MR imaging in the head and neck. *Radiology* 263(1), 19–32 (2012).

12 Vandecaveye V, Dirix P, De Keyzer F *et al*. Predictive value of diffusion-weighted magnetic resonance imaging during chemoradiotherapy for head and neck squamous cell carcinoma. *Eur. Radiol.* 20(7), 1703–1714 (2010).

13 Srinivasan A, Dvorak R, Perni K, Rohrer S, Mukherji SK. Differentiation of benign and malignant pathology in the head and neck using 3T apparent diffusion coefficient values: early experience. *AJNR Am. J. Neuroradiol.* 29(1), 40–44 (2008).

14 Abdel Razek AA, Gaballa G, Elhawarey G, Megahed AS, Hafez M, Nada N. Characterization of pediatric head and neck masses with diffusion-weighted MR imaging. *Eur. Radiol.* 19(1), 201–208 (2009).

15 Vandecaveye V, De Keyzer F, Dirix P, Lambrecht M, Nuyts S, Hermans R. Applications of diffusion-weighted magnetic resonance imaging in head and neck squamous cell carcinoma. *Neuroradiology* 52(9), 773–784 (2010).

16 Bhatia KS, King AD, Yeung DK *et al*. Can diffusion-weighted imaging distinguish between normal and squamous cell carcinoma of the palatine tonsil? *Br. J. Radiol.* 83(993), 753–758 (2010).

17 Maeda M, Kato H, Sakuma H, Maier SE, Takeda K. Usefulness of the apparent diffusion coefficient in line scan diffusion-weighted imaging for distinguishing between squamous cell carcinomas and malignant lymphomas of the head and neck. *AJNR Am. J. Neuroradiol.* 26(5), 1186–1192 (2005).

18 Fong D, Bhatia KS, Yeung D, King AD. Diagnostic accuracy of diffusion-weighted MR imaging for nasopharyngeal carcinoma, head and neck lymphoma and squamous cell carcinoma at the primary site. *Oral Oncol.* 46(8), 603–606 (2010).

19 King AD, Ahuja AT, Yeung DK *et al*. Malignant cervical lymphadenopathy: diagnostic accuracy of diffusion-weighted MR imaging. *Radiology* 245(3), 806–813 (2007).

20 Abdel Razek AA, Soliman NY, Elkhamary S, Alsharaway MK, Tawfik A. Role of diffusion-weighted MR imaging in cervical lymphadenopathy. *Eur. Radiol.* 16(7), 1468–1477 (2006).

21 Sumi M, Sakihama N, Sumi T *et al*. Discrimination of metastatic cervical lymph nodes with diffusion-weighted MR imaging in patients with head and neck cancer. *AJNR Am. J. Neuroradiol.* 24(8), 1627–1634 (2003).

22 Frates MC, Benson CB, Charboneau JW *et al*. Management of thyroid nodules detected at US: Society of Radiologists in Ultrasound Consensus conference statement. *Radiology* 237(3), 794–800 (2005).

23 Razek AA, Sadek AG, Kombar OR, Elmahdy TE, Nada N. Role of apparent diffusion coefficient values in differentiation between malignant and benign solitary thyroid nodules. *AJNR Am. J. Neuroradiol.* 29(3), 563–568 (2008).

24 Erdem G, Erdem T, Muammer H *et al*. Diffusion-weighted images differentiate benign from malignant thyroid nodules. *J. Magn. Reson. Imaging* 31(1), 94–100 (2010).

25 Bozgeyik Z, Coskun S, Dagli AF, Ozkan Y, Sahpaz F, Ogur E. Diffusion-weighted MR imaging of thyroid nodules. *Neuroradiology* 51(3), 193–198 (2009).

26 Aydın H, Kızılgöz V, Tatar Î *et al.* The role of proton MR spectroscopy and apparent diffusion coefficient values in the diagnosis of malignant thyroid nodules: preliminary results. *Clin. Imaging* 36(4), 323–333 (2012).

27 Schueller-Weidekamm C, Kaserer K, Schueller G *et al.* Can quantitative diffusion-weighted MR imaging differentiate benign and malignant cold thyroid nodules? Initial results in 25 patients. *AJNR Am. J. Neuroradiol.* 30(2), 417–422 (2009).

28 Habermann CR, Gossrau P, Graessner J *et al*. Diffusion-weighted echo-planar MRI: a valuable tool for differentiating primary parotid gland tumors? *Rofo* 177(7), 940–945 (2005).

29 Habermann CR, Arndt C, Graessner J *et al*. Diffusion-weighted echo-planar MR imaging of primary parotid gland tumors: is a prediction of different histologic subtypes possible? *AJNR Am. J. Neuroradiol.* 30(3), 591–596 (2009).

30 Ikeda M, Motoori K, Hanazawa T *et al*. Warthin tumor of the parotid gland: diagnostic value of MR imaging with histopathologic correlation. *AJNR Am. J. Neuroradiol.* 25(7), 1256–1262 (2004).

31 Yabuuchi H, Matsuo Y, Kamitani T *et al*. Parotid gland tumors: can addition of diffusion-weighted MR imaging to dynamic contrast-enhanced MR imaging improve diagnostic accuracy in characterization? *Radiology* 249(3), 909–916 (2008).

32 Sumi M, Van Cauteren M, Sumi T, Obara M, Ichikawa Y, Nakamura T. Salivary gland tumors: use of intravoxel incoherent motion MR imaging for assessment of diffusion and perfusion for the differentiation of benign from malignant tumors. *Radiology* 263(3), 770–777 (2012).

33 Sumi M, Van Cauteren M, Nakamura T. MR microimaging of benign and malignant nodes in the neck. *AJR Am. J. Roentgenol.* 186(3), 749–757 (2006).

34 de Bondt RB, Hoeberigs MC, Nelemans PJ *et al*. Diagnostic accuracy and additional value of diffusion-weighted imaging for discrimination of malignant cervical lymph nodes in head and neck squamous cell carcinoma. *Neuroradiology* 51(3), 183–192 (2009).

35 Vandecaveye V, De Keyzer F, Vander Poorten V *et al*. Head and neck squamous cell carcinoma: value of diffusion-weighted MR imaging for nodal staging. *Radiology* 251(1), 134–146 (2009).

36 Perrone A, Guerrisi P, Izzo L *et al*. Diffusion-weighted MRI in cervical lymph nodes: differentiation between benign and malignant lesions. *Eur. J. Radiol.* 77(2), 281–286 (2011).

37 Holzapfel K, Duetsch S, Fauser C, Eiber M, Rummeny EJ, Gaa J. Value of diffusion-weighted MR imaging in the differentiation between benign and malignant cervical lymph nodes. *Eur. J. Radiol.* 72(3), 381–387 (2009).

38 King AD, Tse GM, Ahuja AT *et al*. Necrosis in metastatic neck nodes: diagnostic accuracy of CT, MR imaging, and US. *Radiology* 230(3), 720–726 (2004).

39 Dirix P, Vandecaveye V, De Keyzer F *et al*. Diffusion-weighted MRI for nodal staging of head and neck squamous cell carcinoma: impact on radiotherapy planning. *Int. J. Radiat. Oncol. Biol. Phys.* 76(3), 761–766 (2010).

40 Grégoire V, Coche E, Cosnard G, Hamoir M, Reychler H. Selection and delineation of lymph node target volumes in head and neck conformal radiotherapy. Proposal for standardizing terminology and procedure based on the surgical experience. *Radiother. Oncol.* 56(2), 135–150 (2000).

41 KageiK, Shirato H, Nishioka T *et al*. Ipsilateral irradiation for carcinomas of tonsillar region and soft palate based on computed tomographic simulation. *Radiother. Oncol.* 54(2), 117–121 (2000).

42 Bussels B, Maes A, Hermans R, Nuyts S, Weltens C, Van den Bogaert W. Recurrences after conformal parotid-sparing radiotherapy for head and neck cancer. *Radiother. Oncol.* 72(2), 119–127 (2004).

43 Houweling AC, Wolf AL, Vogel WV *et al*. FDG-PET and diffusion-weighted MRI in head-and-neck cancer patients: implications for dose painting. *Radiother. Oncol.* 106(2), 250–254 (2013).

44 Kim S, Loevner L, Quon H *et al*. Diffusion-weighted magnetic resonance imaging for predicting and detecting early response to chemoradiation therapy of squamous cell carcinomas of the head and neck. *Clin. Cancer Res.* 15(3), 986–994 (2009).

45 Hatakenaka M, Nakamura K, Yabuuchi H *et al*. Pretreatment apparent diffusion coefficient of the primary lesion correlates with local failure in head-and-neck cancer treated with chemoradiotherapy or radiotherapy. *Int. J. Radiat. Oncol. Biol. Phys.* 81(2), 339–345 (2011).

46 King AD, Mo FK, Yu KH *et al*. Squamous cell carcinoma of the head and neck: diffusion-weighted MR imaging for prediction and monitoring of treatment response. *Eur. Radiol.* 20(9), 2213–2220 (2010).

47 Srinivasan A, Chenevert TL, Dwamena BA *et al*. Utility of pretreatment mean apparent diffusion coefficient and apparent diffusion coefficient histograms in prediction of outcome to chemoradiation in head and neck squamous cell carcinoma. *J. Comput. Assist. Tomogr.* 36(1), 131–137 (2012).

48 Thoeny HC, De Keyzer F, Chen F *et al*. Diffusion-weighted magnetic resonance imaging allows noninvasive *in vivo* monitoring of the effects of combretastatin a-4 phosphate after repeated administration. *Neoplasia* 7(8), 779–787 (2005).

49 Chenevert TL, McKeever PE, Ross BD. Monitoring early response of experimental brain tumors to therapy using diffusion magnetic resonance imaging. *Clin. Cancer Res.* 3(9), 1457–1466 (1997).

50 King AD, Chow KK, Yu KH *et al*. Head and neck squamous cell carcinoma: diagnostic performance of diffusion-weighted MR imaging for the prediction of treatment response. *Radiology* 266(2), 531–538 (2013).

51 Galbán CJ, Mukherji SK, Chenevert TL *et al*. A feasibility study of parametric response map analysis of diffusion-weighted magnetic resonance imaging scans of head and neck cancer patients for providing early detection of therapeutic efficacy. *Transl. Oncol.* 2(3), 184–190 (2009).

52 AbdelRazek AA, Kandeel AY, Soliman N *et al*. Role of diffusion-weighted echo-planar MR imaging in differentiation of residual or recurrent head and neck tumors and posttreatment changes. *AJNR Am. J. Neuroradiol.* 28(6), 1146–1152 (2007).

53 Tshering Vogel DW, Zbaeren P, Geretschlaeger A, Vermathen P, De Keyzer F, Thoeny HC. Diffusion-weighted MR imaging including bi-exponential fitting for the detection of recurrent or residual tumour after (chemo)radiotherapy for laryngeal and hypopharyngeal cancers. *Eur. Radiol.* 23(2), 562–569 (2013).

54 Yom SS, Machtay M, Biel MA *et al*. Survival impact of planned restaging and early surgical salvage following definitive chemoradiation for locally advanced squamous cell carcinomas of the oropharynx and hypopharynx. *Am. J. Clin. Oncol.* 28(4), 385–392 (2005).

55 Lambrecht M, Dirix P, Van den Bogaert W, Nuyts S. Incidence of isolated regional recurrence after definitive (chemo-) radiotherapy for head and neck squamous cell carcinoma. *Radiother. Oncol.* 93(3), 498–502 (2009).

56 Nagamachi S, Wakamatsu H, Kiyohara S *et al*. Comparison of diagnostic and prognostic capabilities of ^{18}F-FDG-PET/CT,^{131}I-scintigraphy, and diffusion-weighted magnetic resonance imaging for postoperative thyroid cancer. *Jpn J. Radiol.* 29(6), 413–422 (2011).

57 Ng SH, Chan SC, Yen TC *et al*. Pretreatment evaluation of distant-site status in patients with nasopharyngeal carcinoma: accuracy of whole-body MRI at 3-Tesla and FDG-PET-CT. *Eur. Radiol.* 19(12), 2965–2976 (2009).

58 Ng SH, Chan SC, Yen TC *et al*. Comprehensive imaging of residual/recurrent nasopharyngeal carcinoma using whole-body MRI at 3 T compared with FDG-PET-CT. *Eur. Radiol.* 20(9), 2229–2240 (2010).